Efficient and Robust Automotive Radar Coherent Integration With Range Migration

Oded Bialer, Amnon Jonas, Oren Longman
General Motors - Advanced Technical Center Israel

***Abstract*—Conventional automotive radar perform range-Doppler coherent integration (stretch processing) under the assumption that the range of each object is constant during the integration interval. This assumption yields an efficient computation algorithm. However, when the object's relative speed is high and/or the coherent integration interval is large, the range migration is significant with respect to the range resolution, and as a result, the detection performance of the conventional range-Doppler coherent integration degrades significantly. The Radon-Fourier Transform (RFT) is the optimal method (in the sense of detection performance) for coherent integration with range migration, however, its complexity is large and may not be practical for implementation. In this paper, we develop a range-Doppler coherent integration algorithm that takes into account the range migration with efficient computation. We utilize the fact that range migration is a function of the Doppler frequency and derive an approximation to the RFT. The proposed algorithm significantly outperforms conventional coherent integration when the object's range migration is significant. Furthermore, it attains the performance of the RFT but with significantly lower complexity.**

I. Introduction

Automotive radar is a key sensor for automated driving. One of its main usages is for detection of dynamic vehicles and motorcycles at relatively long distance. The detection at long distance requires a large processing gain, which is achieved by having a relatively long coherent integration interval. On the down side, when the integration time is long and the target vehicle relative speed is large the range of the target migrates significantly (with respect to the range resolution) during the integration interval [1].

Fast chirp FMCW waveform is commonly used in automotive radars [2], [3], since it enables to utilize a large bandwidth (high range resolution) with a low rate analog to digital converter (low power), has high dynamic range, and results in low side-lobes in the ambiguity function along the range domain. In FMCW radar, the received sequence of chirps are multiplied by the transmitted reference chirps, which results in a sequence of down-converted chirps. Conventionally, range-Doppler stretch processing is done by 2D fast Fourier transform (FFT) on the sequence of down converted chirps [4]-[5], where the sequence length is the coherent integration duration. The conventional 2D FFT stretch processing is efficient in terms of computation complexity, and is the exact matched filter processing that achieves maximal signal-to-noise ratio (SNR) under the assumption that the target's range and Doppler are constant during the integration interval.

State-of-the-art automotive radars [6] have a range resolution of about $10cm$, and in order to detect targets at long range they have a coherent integration duration of about $20ms$ (which is required to obtain sufficient SNR). Under these settings, the assumption of constant Doppler frequency during the coherent integration interval holds, however, the range migrates significantly (with respect to the radar's range resolution) in the case of fast moving targets. For example when the relative speed is $100kph$ then the range migration over $20ms$ is $55cm$, which is larger than five times the range resolution. In this case the 2D FFT stretch processing results in a significant degradation in the target SNR, which reduces the detection probability of the target. Furthermore, even if the target is detected it is smeared over several range resolution cells, which reduces the accuracy of the estimated target range.

One approach to overcome this problem, is to apply the Radon-Fourier transform (RFT) [7] instead of the 2D FFT. The RFT achieves maximum SNR even when there is range migration, however, it has significantly higher complexity than 2D FFT (as will be shown in Section III), and therefore may be impractical for implementation in production automotive radars. Xu at el. [8] have proposed to apply conventional 2D FFT to detect the targets and obtain a coarse estimation of the targets parameters. Then the targets parameters are refined by applying coherent integration for each individual target while compensating for the range migration based on the initial estimated target parameters. This approach is computational efficient with respect to the RFT, and improves the accuracy of the estimated target range and Doppler compared to 2D FFT stretch processing. However, since it primarily relies on conventional 2D FFT stretch processing to detect the targets it suffers from degraded detection performance in the presence of range migration.

In this paper, we develop a range-Doppler coherent integration algorithm that takes into account the range migration with efficient computation. We analyze the performance (range estimation accuracy and detection probability) and complexity of the proposed algorithm compared to conventional 2D FFT stretch processing and to RFT, which has optimal matched filter performance. The developed algorithm achieves the performance of RFT and attains a significant performance advantage over conventional 2D FFT when the targets have range migration. It has significantly lower computation complexity than RFT and requires a modest increase in complexity with respect to 2D FFT, and thus it is practical for implementation in automotive radar systems.

II. System Model and Problem Definition

A fast chirp FMCW automotive radar [2], [3] is considered. The sequence of transmitted chirps can be expressed by

$$x(t) = \sum_{m=0}^{M-1} s(t - mT_c) \ , \tag{1}$$

where T_c is the chirp duration, M is the number of chirps in the coherent processing frame, and

$$s(t) = \begin{cases} e^{-j2\pi(f_c t + \frac{1}{2}\alpha t^2)}, & \text{if } 0 \le t \le T_c \\ 0, & \text{otherwise} \ , \end{cases} \tag{2}$$

is a single chirp, where f_c is the carrier frequency and α is the chirp slope.

The received reflected sequence of FMCW chirps are down converted by multiplication with the conjugate transmitted signal. The resulting sampled down converted chirps for a single point reflector with unit intensity can be expressed by

$$y[n,m] = e^{j2\pi\alpha t_0 n T_s} e^{j2\pi f_d m T_c} e^{j2\pi\alpha\frac{f_d}{f_c}(nT_s + mT_c)nT_s}, \tag{3}$$

where f_d is the reflection point Doppler frequency, T_s is the sampling interval, t_0 is the round trip propagation delay (from the radar to the reflection point and back), $n = 0, 1, .., N-1$, is the index of a sample within a chirp, and $m = 0, 1, .., M-1$, is the chirp index.

The signal $y[n,m]$ is comprised of three exponents, the first exponent consists of linear phase shift within each chirp that is related to the target's range at the beginning of the integration interval (t_0). The second exponent is the phase shift along chirps related to the Doppler frequency f_d, and the third exponent is the phase rotation due to the range migration within chirps and along chirps.

Conventionally, it is assumed that the target range migration along the sequence of chirps is negligible and hence the argument, $\alpha(\frac{f_d}{f_c}(nT_s + mT_c)))T_s n$, in the third exponent in (3) is neglected. Under this assumption stretch processing is performed on $y[n,m]$ by a 2D FFT. Where the first dimension operates per chirp over index n, and the second dimension along chirps over index m. The resulting rang-Doppler stretch processing is given by

$$\hat{Y}[k,l] = \sum_{m=0}^{M-1}\sum_{n=0}^{N-1} y[n,m] e^{-j2\pi k\frac{n}{N}} e^{-j2\pi l\frac{m}{M}} \ , \tag{4}$$

where k, and l, are the range and Doppler bin indexes, respectively. As mentioned in Section I, the 2D FFT stretch processing has degraded SNR and smeared range when the targets speed is high with respect to the radar's range resolution.

The Radon-Fourier transform (RFT) is the exact matched filter processing in the presence of range migration, and it is given by

$$Y[k,l] = \sum_{m=0}^{M-1}\sum_{n=0}^{N-1} y[n,m] e^{-j2\pi l\frac{\alpha}{f_c}(\frac{nT_s}{T_c M} + \frac{m}{M})nTs} e^{-j2\pi k\frac{n}{N}} e^{-j2\pi l\frac{m}{M}} \ . \tag{5}$$

The RFT attains the maximal SNR, however the complexity of calculating (5) for $k = 0, 1, .., N-1$ range bins and $l = 0, 1.., M-1$ Doppler bins is $O(N^2M^2)$. On the other hand, the conventional 2D FFT stretch processing has complexity of $O(MN(log(N) + log(M)))$, which is about MN times smaller when M and N are relatively large (as is typically the case). However the reduced complexity comes with a performance degradation. The problem at hand is to develop a range-Doppler coherent integration algorithm that achieves the RFT performance when there is range migration but with significantly lower complexity.

III. Coherent Integration Algorithm

In this section, we derive a coherent integration algorithm that approximates the RFT in (5) with less computational complexity. We first neglect the minor range migration within the chirp duration. Under this assumption we can express (5) as

$$Y[k,l] = \sum_{m=0}^{M-1}\sum_{n=0}^{N-1} y[n,m] e^{-j2\pi l\frac{\alpha}{f_c}\frac{m}{M}nT_s} e^{-j2\pi k\frac{n}{N}} e^{-j2\pi\frac{l}{M}m}. \tag{6}$$

Define the discrete time Fourier transform (DTFT) at frequency f of the sequence $y[n,m]$ for $n = 0, 1, .., N-1$, as

$$\tilde{U}[f,m] = \sum_{n=0}^{N-1} y[n,m] e^{-j2\pi f T_s n}. \tag{7}$$

By substituting (7) into (6) we have that

$$Y[k,l] = \sum_{m=0}^{M-1} \tilde{U}\left[\frac{k + \Delta(l,m)}{NT_s}, m\right] e^{-j2\pi\frac{l}{M}m}, \tag{8}$$

where $\Delta(l,m) = l\frac{\alpha}{f_c}\frac{m}{M}NT_s$.

We approximate that the amplitude of the DTFT at a non-integer frequency index, $k+\Delta(l,m)$, is close to the amplitude of the DTFT at the integer bin that is closest to $k + \Delta(l,m)$ since their frequency difference is small, i.e.,

$$\left|\tilde{U}\left[\frac{k + \Delta(l,m)}{NT_s}, m\right]\right| \approx \left|\tilde{U}\left[\frac{k + \lfloor\Delta(l,m)\rceil}{NT_s}, m\right]\right|, \tag{9}$$

where $\lfloor x\rceil$ is the closest integer value of x (round operation). Under the approximation in (9) we have that

$$\begin{aligned} &\tilde{U}\left[\frac{k + \Delta(l,m)}{NT_s}, m\right] = \\ &\left|\tilde{U}\left[\frac{k + \Delta(l,m)}{NT_s}, m\right]\right| e^{j\angle\tilde{U}\left[\frac{k+\Delta(l,m)}{NT_s}, m\right]} \approx \\ &\left|\tilde{U}\left[\frac{k + \lfloor\Delta(l,m)\rceil}{NT_s}, m\right]\right| e^{j\angle\tilde{U}\left[\frac{k+\Delta(l,m)}{NT_s}, m\right]} = \\ &\tilde{U}\left[\frac{k + \lfloor\Delta(l,m)\rceil}{NT_s}, m\right] e^{j\phi(k,l,m)}, \end{aligned} \tag{10}$$

where

$$\phi(k,l,m) = \angle\tilde{U}\Big[\frac{k + \Delta(l,m)}{NT_s}, m\Big] - \angle\tilde{U}\Big[\frac{k + \lfloor\Delta(l,m)\rceil}{NT_s}, m\Big], \tag{11}$$

and $\angle x$ denotes the phase of x.

Denote $U[k,m]$ as the k^{th} bin of the discrete Fourier transform (DFT) of the sequence $y[n,m]$ for $n = 0, 1, .., N-1$, i.e.,

$$U\left[k,m\right] = \sum_{n=0}^{N-1} y[n,m] e^{-j2\pi \frac{k}{N} n}. \quad (12)$$

Note that $\tilde{U}\left[\frac{k+\lfloor\Delta(l,m)\rceil}{NT_s}, m\right]$ is the DFT of $y[n,m]$ at bin $k+\lfloor\Delta(l,m)\rceil$, thus

$$\tilde{U}\left[\frac{k+\lfloor\Delta(l,m)\rceil}{NT_s}, m\right] = U\Big[k + \lfloor\Delta(l,m)\rceil, m\Big]. \quad (13)$$

By substituting (13) into (10) and then the result into (8) we obtain that

$$Y[k,l] \approx \sum_{m=0}^{M-1} U\left[k+\lfloor\Delta(l,m)\rceil, m\right] e^{-j\left(2\pi \frac{l}{M} m - \phi(k,m,l)\right)}. \quad (14)$$

Next, we derive the expression for $\phi(k,m,l)$. By substituting (3) into (7), and neglecting the range migration within the chirp we have that

$$\tilde{U}\left[f,m\right] = e^{j2\pi f_d m T_c} \sum_{n=0}^{N-1} e^{j2\pi(\alpha t_0 + \alpha \frac{f_d}{f_c} m T_c - f) n T_s}. \quad (15)$$

Replacing the summation in (15) by the known identity (see (4.2.49) in [9])

$$\sum_{n=0}^{N-1} e^{j\omega n} = \frac{\sin(\omega N/2)}{\sin(\omega/2)} e^{j\omega(N-1)/2}, \quad (16)$$

with $\omega = 2\pi(\alpha t_0 + \alpha \frac{f_d}{f_c} m T_c - f) T_s$, and then substituting the result into (11) yields that

$$\phi(k,m,l) = \pi\left(\frac{N-1}{N}\right)\Big(\Delta(l,m) - \lfloor\Delta(l,m)\rceil\Big), \quad (17)$$

where $\phi(k,m,l)$ is independent of k. Finally, by substituting (17) into (14) we obtain a simplified approximation to the RFT, which is given by

$$Y[k,l] \approx \sum_{m=0}^{M-1} U\left[k+\lfloor\Delta(l,m)\rceil, m\right] \cdot e^{-j2\pi\left(\frac{l}{M} m - \frac{N-1}{2N}(\Delta(l,m) - \lfloor\Delta(l,m)\rceil)\right)}. \quad (18)$$

The proposed coherent combining in (18) can be interpreted as a modified DFT hence we refer to it as range migration DFT (RMDFT). THE RMDFT can be efficiently computed as follows. First, compute the conventional range stretch processing by FFT on the samples of each individual down converted chirp, which results in $U[k,m]$ for $k = 0, .., N-1$, and $m = 0, .., M-1$. Second, obtain Doppler stretch processing per each range bin index k and Doppler bin index l, by selecting the sequence of range bins $U[k+\lfloor\Delta(l,m)\rceil]$ for chirps $m = 0, .., M-1$, and coherently combining them with the phase argument in the exponent of (18), which is a function of the Doppler bin. The pseudo code of the algorithm is described in Algorithm 1.

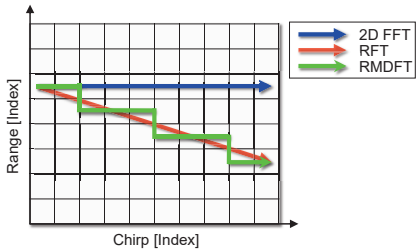

Fig. 1: Range-Doppler stretch processing methods.

Process	Complexity	Ratio W.R.T 2D FFT
2D FFT	$O(NM(\log(N)+\log(M)))$	
RFT	$O(N^2M^2)$	$O(\frac{NM}{\log(M)})$
RMDFT	$O(NM(\log(N)+M))$	$O(\frac{M}{\log(M)})$

TABLE I: Complexity of stretch processing methods.

Fig. 1 illustrate the difference between the conventional 2D FFT stretch processing, RFT and the proposed RMDFT. Each column in the grid map of the figure represents the range FFT output of a different chirp. In conventional stretch processing, the range is constant along chirp (blue curve). In RFT, the range migrates continuously along the chirps (red plot), and in RMDFT (green plot) the range migrates in steps due to the quantization of the range migration to integer range bin indexes. The offset in the range bin samples between the red and green result in an amplitude and phase offset. The amplitude offset is neglected and the phase offset is compensated by the term $\phi(k,m,l)$.

As for the complexity of RMDFT. Considering the case that the number of range bins is equal to the number of samples per chirp, N, and the number of Doppler frequency bins is equal to the number of chirps, M. The complexity of computing the range stretch processing by FFT for each chirp is $O(MNlog(N))$. The complexity of computing the Doppler stretch processing for M Doppler bins per each range bin is $O(NM^2)$. Hence the total complexity of the proposed RMDFT is $O(NM(\log(N)+M))$. The computational complexities of the conventional 2D FFT range-Doppler stretch processing, RFT and RMDFT are summarized in Table I. The complexity of RMDFT is $M/log(M)$ times higher than conventional 2D FFT stretch processing, and by a factor of N smaller than RFT. Typically in automotive radar N and M are in the range $(256-2048)$, hence the complexity reduction of RMDFT with respect to RFT is significant.

IV. Performance Evaluation

In this section we evaluate the performance of the proposed method using simulation and real radar field experiment.

A. Simulation tests

For the simulation tests we used the following radar parameters. Carrier frequency of 77GHz, bandwidth of 1GHz, chirp duration of $T_c = 35\mu s$, single Rx and Tx channels, sampling frequency of $1/T_s = 22.2$MHz, and relatively long coherent integration duration of $72ms$ with $M = 2048$ chirps.

Algorithm 1 Range Migration DFT (RMDFT)

Input: $y[n,m]$, $n=0,1,..,N-1$, $m=0,1,..,M-1$
Output: $Y[k,l]$, $k=0,1,..,K-1$, $l=0,1,..,L-1$
Initialization:
% Calculate modified Doppler DFT matrix
for $m=0:M-1$ **do** ▷ Loop on chirps
  for $l=0:L-1$ **do** ▷ Loop on Dopplers
    $\boldsymbol{D}[m,l]=e^{-j2\pi\left(\frac{l}{M}m-\frac{N-1}{2N}(\Delta(l,m)-\lfloor\Delta(l,m)\rceil)\right)}$
  end for
end for
Coherent integration computation:
% Perform range FFT per chirp
for $m=0:M-1$ **do** ▷ Loop on chirps
  $\boldsymbol{U}[:,m]=\text{FFT}(y[:,m])$
end for
% Perform Doppler DFT with range migration
for $k=0:K-1$ **do** ▷ Loop on range bins
  for $l=0:L-1$ **do** ▷ Loop on Doppler
    $\boldsymbol{r}=zeros(M,1)$
    for $m=0:M-1$ **do** ▷ Loop on chirps
      $\boldsymbol{r}[m]=\boldsymbol{U}[k+\lfloor\Delta(l,m)\rceil,m]$
    end for
    % Multiply with modified Doppler DFT module
    $Y[:,l]=\boldsymbol{r}^T\boldsymbol{D}[:,l]$
  end for
end for

For all the tests in this section we simulated a scenario with a point target in front of the radar at range $29.75m$ that moves towards the radar at speed of $187kph$. In this setting the range migration over the coherent integration duration of $72msec$ is $3.7m$, while the radar's range resolution is $15cm$.

Fig. 2a presents the range FFT output per chirp. The y-axis is the range FFT and the x-axis is the chirp index. The figure shows that the range migration is significant with respect to the main lobe width of the range FFT output (the range resolution).

Fig. 2b, presents the result of the conventional range-Doppler 2D FFT stretch processing. Fig. 2c shows the range-Doppler stretch processing of the proposed RMDFT (Algorithm 1). The correct target range and Doppler is marked by a white cross in both figures. It is clearly seen that the range-Doppler main-lobe spread in the case of RMDFT is significantly smaller than in the case of the conventional stretch processing. Moreover, the center of the peak in the range-Doppler spectrum of RMDFT is at the correct target range and Doppler (white cross), while the main-lobe peak in the conventional stretch processing has an offset in range and Doppler with respect to the correct target range and Doppler.

Fig. 2d shows the range cut at the Doppler frequency of the peak in each one of the range-Doppler images in Fig. 2b and Fig. 2c. The blue plot is the range cut of RMDFT and the red plot is the range cut of the conventional stretch processing. For reference we also add the range cut of the RFT (black dashed plot). It is realized that the result of RMDFT is similar to the RFT, and both obtain a higher intensity with narrow spread in the vicinity of the target compared to the conventional 2D FFT stretch processing.

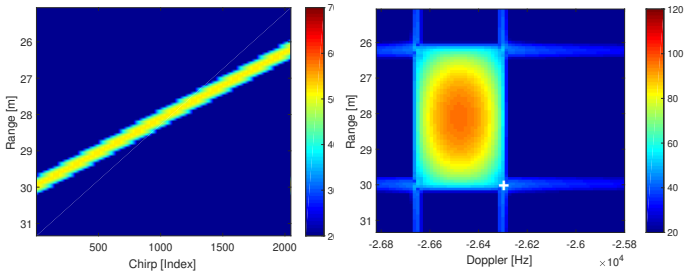

(a) Range FFT output (y-axis) vs. chirp index (x-axis)

(b) Range-Doppler spectrum of 2D FFT stretch processing

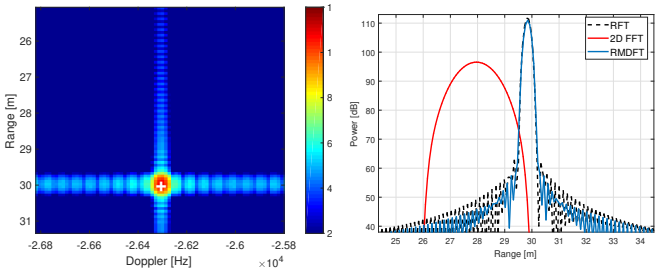

(c) Range-Doppler spectrum of RMDFT

(d) Range cut at target's Doppler of stretch processing algorithms

Fig. 2: Stretch processing performance for dynamic target.

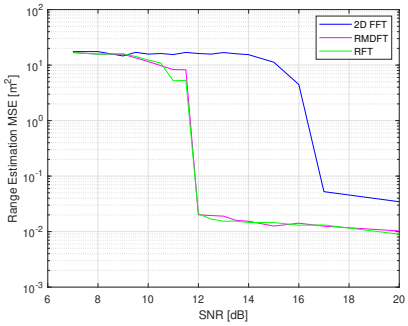

Fig. 3: Range estimation MSE.

Figs. 3-4 presents the range estimation mean square error (MSE) and Doppler MSE vs. SNR for the test scenario of a single point reflector. There were 1000 Monte Carlo experiments per each SNR point. In each experiment, the estimated range was the range of the range-Doppler spectrum peak. The MSE of the proposed method is similar to the MSE of RFT, and both achieve the same performance as the conventional stretch processing with 5 dB less SNR. Fig. 5 presents the receiver operating characteristic (ROC) of RMDFT, RFT, and the conventional 2D FFT stretch processing for the case of a point reflector with 13 dB SNR. The detection performance of RMDFT are similar to RFT and both are significantly better than the conventional stretch processing.

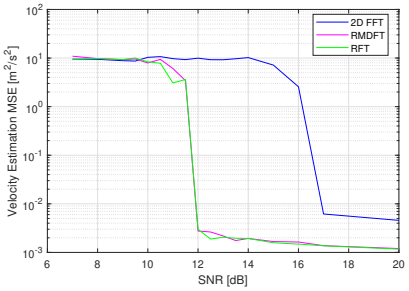

Fig. 4: Doppler estimation MSE.

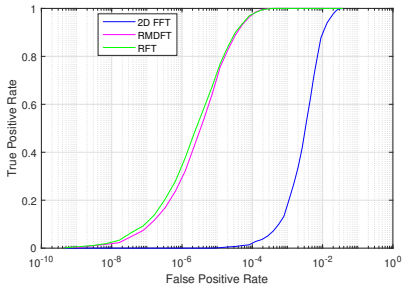

Fig. 5: ROC for point target with 13dB SNR.

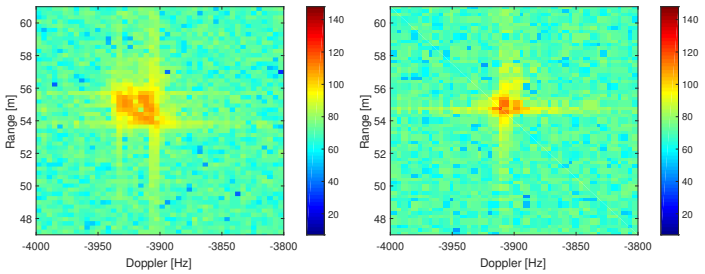

(a) Range-Doppler spectrum of 2D FFT stretch processing.

(b) Range-Doppler spectrum of RMDFT.

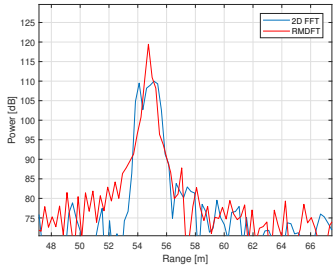

(c) Range cut at target's Doppler bin of Fig. 6a (blue) and Fig. 6b (red).

Fig. 6: RMDFT and conventional 2D FFT stretch processing results for real radar measurements of a vehicle target.

B. Radar experiment

The performance of the proposed methods was also evaluated in a field experiment using an automotive $77GHz$ radar. The radar had a chirp duration of $T_c = 35\mu s$, bandwidth of 1GHz, sampling frequency of $1/T_s = 25$MHz, and a long integration duration of 230ms. In the test scenario there was a target vehicle that was moving towards the radar at low speed of 36kph. The range migration in this case was 2.3m, which is severe with respect to the range resolution, which was 15cm.

The range-Doppler stretch processing results of the conventional 2D FFT processing and RMDFT for this test case, are presented in Fig. 6a, and Fig. 6b, respectively. The corresponding range cut at the Doppler of the peak for these two images is shown in Fig. 6c. It is realized that similar to the results in the simulation, the proposed algorithm attains a relatively narrow spread in the range-Doppler spectrum, and even more importantly, achieves about $10dB$ higher SNR than conventional processing (as observed in Fig. 6c).

V. Conclusion

In this paper, we developed a coherent integration algorithm for a fast chirp FMCW automotive radar that is robust to range migration during the integration interval and is efficiently computed. The performance of the method was evaluated with simulation and real radar measurements. The algorithm attains a significant performance advantage in the probability of detection and in the MSE of the range and Doppler estimation compared to conventional stretch processing when the range migration is significant with respect to the range resolution. Furthermore, it attains the performance of the Fourier-Radon Transform, which is optimal in the sense of maximal SNR, but with the advantage that it has significantly lower computational complexity and thus is practical for implementation. The proposed algorithm can accurately detect targets with high speed at long distance by exploiting the SNR gain of long integration duration and large radar bandwidth (which provides high range resolution) without suffering from performance degradation due to range migration.

References

[1] O. Longman and I. Bilik, "Spectral Radon–Fourier transform for automotive radar applications," *IEEE Transactions on Aerospace and Electronic Systems*, vol. 57, no. 2, pp. 1046–1056, 2020.

[2] Z. Tong, R. Renter, and M. Fujimoto, "Fast chirp FMCW radar in automotive applications," in *IET International Radar Conference*, pp. 1–4, IET, 2015.

[3] O. Bialer, A. Jonas, and T. Tirer, "Code optimization for fast chirp FMCW automotive MIMO radar," *IEEE Transactions on Vehicular Technology*, vol. 70, no. 8, pp. 7582–7593, 2021.

[4] R. Wan, Y. Song, T. Mu, and Z. Wang, "Moving target detection using the 2D-FFT algorithm for automotive FMCW radars," in *International Conference on Communications, Information System and Computer Engineering (CISCE)*, pp. 239–243, IEEE, 2019.

[5] I. Bilik, O. Bialer, S. Villeval, H. Sharifi, K. Kona, M. Pan, D. Persechini, M. Musni, and K. Geary, "Automotive MIMO radar for urban environments," in *IEEE Radar Conference (RadarConf)*, pp. 1–6, IEEE, 2016.

[6] I. Bilik, et al., "Automotive multi-mode cascaded radar data processing embedded system," *IEEE Radar Conference*, pp. 372–376, 2018.

[7] J. Xu, J. Yu, Y.-N. Peng, and X.-G. Xia, "Long-time coherent integration for radar target detection base on Radon-Fourier transform," in *IEEE Radar Conference*, pp. 432–436, IEEE, 2010.

[8] Z. Xu, C. J. Baker, and S. Pooni, "Range and Doppler cell migration in wideband automotive radar," *IEEE Transactions on Vehicular Technology*, vol. 68, no. 6, pp. 5527–5536, 2019.

[9] J. G. Proakis and D. G. Manolakis, "Digital signal processing," 4^{th} *Edition, Pearson Education India*, 2007.